RSC Advances

PAPER

View Article Online
View Journal | View Issue

Cite this: *RSC Adv.*, 2022, **12**, 25457

A simple protocol for determination of enantiopurity of amines using BINOL derivatives as chiral solvating agents *via* ^{1}H- and ^{19}F-NMR spectroscopic analysis†

Pooja Chaudhary,[a] Geeta Devi Yadav[b] and Surendra Singh *[a]

A rapid and simple protocol for the determination of enantiopurity of primary and secondary amines was developed by using (*S*)-BINOL/(*S*)-BINOL derivatives/(*R*)-1,1′-binaphthyl-2,2′-diyl hydrogenphosphate as chiral solvating agents *via* ^{1}H- and ^{19}F-NMR spectroscopic analysis. In this protocol, the analyte and chiral solvating agent were directly mixed in an NMR tube in chloroform-*d* and after shaking for 30 seconds the ^{1}H- and ^{19}F-NMR spectra were recorded, which affords well-resolved resonance peaks for both the enantiomers present in an analyte. The enantiomeric excess of 1,2-diphenylethylenediamine was determined and linear relationship with coefficient of R^2 = 0.9995 was observed. The binding constant and associated Δ*G* values were also calculated for diastereomeric complexes formed between both the enantiomers of analyte **5** with CSA (*S*)-**3a** by using UV-visible spectroscopy.

Received 23rd August 2022
Accepted 25th August 2022

DOI: 10.1039/d2ra05291a

rsc.li/rsc-advances

Introduction

Extraordinary development in asymmetric synthesis provided easy entrance to various classes of chiral compounds. Chiral compounds are important building blocks in the biochemistry and pharmaceutical industry. Therefore, the enantiodifferentiation and awareness of enantiomeric excess are extremely essential in several areas such as catalysis, pharmacology, asymmetric synthesis, and biochemistry.[1–5] Among all organic compounds used in the pharmaceutical industry, chiral amines are in high demand because of their application as chiral building blocks in drug discovery and their broad range of biological activities.[6,7] The most extensively used methods to determine the enantiopurity of chiral compounds are circular dichroism (CD), optical rotation, high-performance liquid chromatography (HPLC), and gas chromatography (GC).[8–13] The measurement of optical purity by optical rotation and circular dichroism (CD) is easy and inexpensive but the results obtained are dependent on various parameters like amount, temperature, solvent, and the presence of impurities in the sample. HPLC and GC provided the accurate measurement of enantiomeric purity of chiral compounds but they required expensive chiral columns and HPLC solvents.

The fast HPLC methods[14,15] and supercritical fluid chromatography (SFC)[16] already reported as efficient techniques for rapid enantiopurity determination of chiral compounds but it has been always in demand to develop a simple and rapid protocol to determine the enantiopurity and absolute configuration of synthesized chiral products. In the last few decades, the measurement of enantiomeric excess by nuclear magnetic resonance (NMR) spectroscopy has already been reported as a rapid and reliable protocol in the literature.[17–37] The determination of enantiopurity *via* NMR spectroscopy required the presence of a chiral auxiliary to convert the enantiomers into diastereomers. The most commonly used chiral auxiliaries are chiral solvating agents {CSAs like tyrosine-modified pillar[5]arenes, *R*-VAPOL-phosphoric acid, organic-soluble acids, benzene tricarboxamide-based hydrogelators, BINOL phosphoric acid, Kagan's amides, roof-shape amines, BINOL and its derivatives},[17–31] chiral derivatizing agents {CDAs like Δ-$[Ir(ppy)_2(MeCN)_2](PF_6)$ (ppy is 2-phenylpyridine), α-methoxy-α-phenylacetic acid (MPA), α-methoxy-α-trifluoromethylphenylacetic acid (MTPA) and BINOL},[31–36] chiral lanthanide shift reagents {CLSRs like $[Eu(tfc)_3]$, $[Eu(hfc)_3]$, $[Sm(tfc)_3]$, and [(*R*)-$Pr(tfc)_3$]}.[37–39] Among all the chiral auxiliaries reported for NMR chiral recognition, BINOL and its derivatives represent a useful auxiliary because of their direct utilization as a CSA. The BINOL and its derivatives are reported as a chiral solvating agent for NMR enantiodifferentiation of amines,[26] promethazine,[27] alkaloid crispine A,[28] isoflavones,[40] sulfinimines,[41] omeprazole,[42] and flavones.[43]

The nature of solvent is also important for this type of chiral analysis because the anisochrony observed between

[a]*Department of Chemistry, University of Delhi, Delhi-110007, India. E-mail: ssingh1@chemistry.du.ac.in*

[b]*Department of Chemistry, Swami Shraddhanand College, University of Delhi, Delhi-110036, India*

† Electronic supplementary information (ESI) available. See https://doi.org/10.1039/d2ra05291a

diastereomeric host–guest complexes is preeminent in non-polar deuterated solvents like CCl_4, $CDCl_3$, and C_6D_6. While polar solvents like acetonitrile-d_3, acetone-d_6, and methanol-d_4 preferentially solvate the analyte (guest) and the enantiodifferentiation ($\Delta\delta^{R/S}$) of analyte falls to zero.[44] This explains the importance of intermolecular hydrogen bond formation between CSA and analyte to form the diastereomeric complexes.

Bull and James reported the enantiopurity determination of amine **5** using (*R*)-BINOL as an effective chiral derivatizing agent with 2-formylphenylboronic acid. In that case, chiral BINOL undergoes the enantiodifferentiation of amine **5** by forming diastereomeric iminoboronate ester complexes *via* covalent (strong) interactions.[35] The chemical shift difference value obtained with Bull and James protocol is higher but it is not easy to recovered and purify the BINOL from the system for reusing it in next experiment.

In this manuscript, we report a complete assessment of the effectiveness of (*S*)-BINOL (**1**), 3,3′-disubstituted (*S*)-BINOLs (**2** and **3a–d**), and (*R*)-1,1′-binaphthyl-2,2′-diyl hydrogenphosphate (**4**) as chiral solvating agents for the enantiodifferentiation of various types of amines (**5-11**) *via* ^{1}H- and ^{19}F-NMR spectroscopic analysis (Fig. 1). In this protocol, the enantiodifferentiation of amine **5** is based on the principle that enantiomers of amine **5** (guest) complexed with CSA (*S*)-**3a** (host) through non-covalent (weak) interactions[30] such as hydrogen bonding, π–π interactions to form two diastereomeric host–guest complexes, as a result different chemical shift values observed for both the enantiomers of amine **5** in ^{1}H-NMR spectrum. Herein, the chiral solvating agent (*S*)-**3a** can be easily purified by column chromatography and reused for the next experiments.

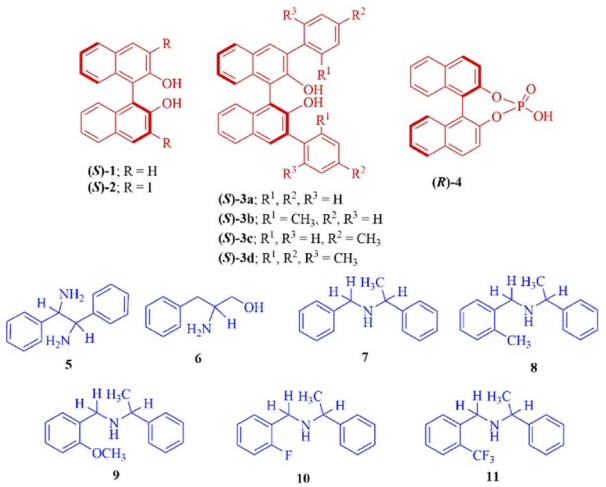

Fig. 1 The (*S*)-BINOL (**1**), 3,3′-disubstituted (*S*)-BINOLs (**2 and 3a–d**) and (*R*)-1,1′-binaphthyl-2,2′-diyl hydrogenphosphate (**4**) as a chiral solvating agents (CSAs) (red colour) and different types of amines as analytes (blue colour).

Results and discussion

The 3,3′-disubstituted (*S*)-BINOLs (**2** and **3a–d**) were synthesized from (*S*)-BINOL (>99% *ee*) according to Scheme 1. The hydroxy group of (*S*)-BINOL was protected as methoxymethyl (MOM) ether using sodium hydride and methoxymethyl chloride by following the reported procedure.[45] The direct *ortho*-lithiation of MOM-protected (*S*)-BINOL (**12**) using *n*-BuLi followed by quenching with iodine afforded the 3,3′-diiodo substituted MOM-protected (*S*)-BINOL (**13**) in 75% yield.[46] The Suzuki coupling reaction of diiodide (**13**) with various boronic acids such as phenylboronic acid, *ortho*-tolylboronic acid, *para*-tolylboronic acid, and 2,4,6-trimethylphenylboronic acid, catalyzed by $Pd(PPh_3)_4$, afforded the corresponding 3,3′-disubstituted MOM-protected (*S*)-BINOLs (**14a–d**) in 76–85% yields.[47] Further, deprotection of 3,3′-disubstituted MOM-protected (*S*)-BINOLs (**14a–d**) under acidic conditions afforded the 3,3-disubstituted (*S*)-BINOLs (**3a–d**) in 96–98% yields.[48] 3,3′-Diiodo (*S*)-BINOL (**2**) was also obtained in 98% yield after

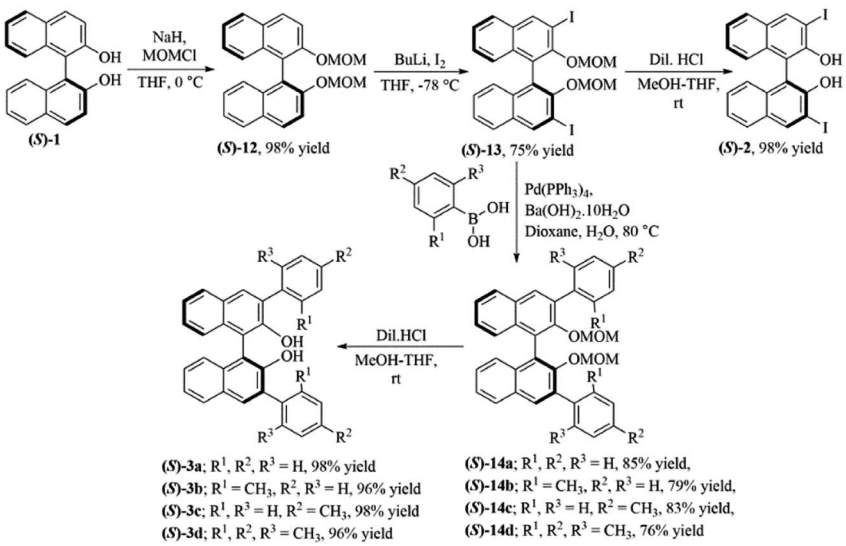

Scheme 1 Synthesis of 3,3′-disubstituted (*S*)-BINOLs (**2** and **3a–d**) from (*S*)-BINOL (**1**).

deprotection of 3,3′-diiodo MOM-protected (*S*)-BINOL (**13**) under acidic conditions.[48] All of the reported 3,3′-disubstituted (*S*)-BINOLs (**2**, **3a–d**) were characterized by ^{1}H- and ^{13}C-NMR spectroscopy. The optical purity of these 3,3′-disubstituted (*S*)-BINOLs was confirmed by comparing their optical rotation values with the reported literature.[49]

The enantiopure amine **5** is a valuable chiral source for the synthesis of chiral ligands and organocatalysts.[50–52] The enantiopurity of chiral amine **5** can be determined by HPLC after its derivatization but it takes a lot of time, whereas by using this protocol it can be determined in five minutes (including the sample preparation time). Initially, enantiodifferentiation of *rac*-**5** was carried by using 0.1 mmol of MOM-protected (*S*)-BINOL (**12**)/3,3′-diiodo-MOM-protected (*S*)-BINOL (**13**) in 0.6 mL chloroform-*d* at 25 °C. In the absence of CSAs, the CH resonance of *rac*-**5** appeared at δ = 4.10 ppm (singlet signal) and with MOM-protected (*S*)-BINOLs **12** and **13** no change was observed in singlet signal of *rac*-**5**, this may be due to the absence of hydrogen bonding interaction between CSAs (**12** and **13**) and analyte **5** (Table 1, entries 1 and 2 and Fig. 2). Later, the (*S*)-BINOL and its derivatives **1**, **2**, and **3a–d** were tested as CSAs and it was observed that the singlet signal for CH proton of *rac*-**5** split into two discrete resonance peaks with a chemical shift difference ($\Delta\delta^{R/S}$) values of 0.02 to 0.06 ppm (Table 1, entries 3–8 and Fig. 2). This may be due to intermolecular hydrogen bond formation between OH and NH_2 groups of (*S*)-BINOLs and *rac*-**5**, respectively. It was also observed that the proton signal for OH group of (*S*)-BINOLs was upfield shifted while for NH_2 group of *rac*-**5** downfield shifted and merged as a broad singlet signal, which also confirms the intermolecular hydrogen bonding interactions between (*S*)-BINOLs and *rac*-**5**.[53]

Table 1 Screening of various chiral solvating agents (CSAs) to determine the enantiodifferentiation of *rac*-**5**[a]

Entry	(CSAs)	Chemical shift difference ($\Delta\delta^{R/S}$)[b] (ppm)
1	(*S*)-**12**	No resol.
2	(*S*)-**13**	No resol.
3	(*S*)-**1**	0.02
4	(*S*)-**2**	0.03
5	(*S*)-**3a**	0.06
6	(*S*)-**3b**	0.03
7	(*S*)-**3c**	0.04
8	(*S*)-**3d**	0.02

[a] In NMR tube, the CSAs (0.1 mmol) and *rac*-**5** (0.05 mmol) were dissolved in chloroform-*d* (0.6 mL) and after shaking the NMR tube for 30 seconds, ^{1}H-NMR spectrum was recorded on a 400 MHz NMR spectrometer at 25 °C. [b] Calculated from the ^{1}H-NMR spectrum.

The maximum enantiodifferentiation observed with (*S*)-**3a**, indicates the stronger hydrogen bonding interactions between NH_2 and OH group of *rac*-**5** and (*S*)-**3a**, respectively. The better results obtained with (*S*)-**3a** as compared to other 3,3′-disubstituted (*S*)-BINOLs may be due to extra stabilization of hydrogen bonding interactions by π–π stacking interactions between phenyl rings of *rac*-**5** and (*S*)-**3a**. While for other 3,3′-disubstituted (*S*)-BINOLs (**2** and **3b–d**), no π–π stacking interactions possible due to the presence of bulky methyl group(s) on phenyl ring and iodide group on these BINOLs. These results reveal that the chemical shift difference ($\Delta\delta^{R/S}$) value is dependent on optimal host–guest complexation, which arise from the appropriate substitution in the chiral solvating agents (CSAs).

After assessing the various chiral solvating agents (CSAs), the typical experiments were conducted to optimize the amounts of (*S*)-**3a** and *rac*-**5**. ^{1}H-NMR spectra of *rac*-**5** (0.05 mmol) were

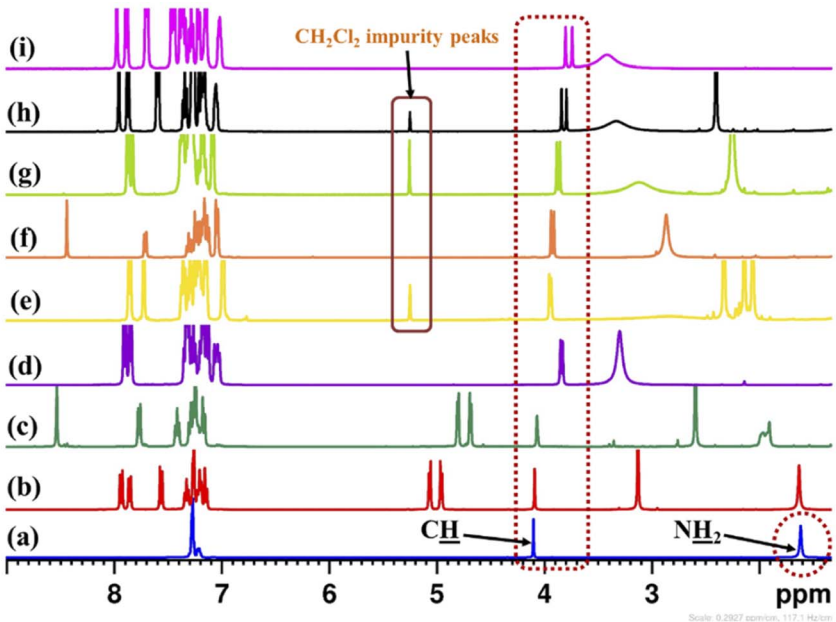

Fig. 2 Partial stacked plot of ^{1}H-NMR spectrum (400 MHz, $CDCl_3$) of (a) neat *rac*-**5**, (b) *rac*-**5** with (*S*)-**12**, (c) *rac*-**5** with (*S*)-**13**, (d) *rac*-**5** with (*S*)-**1**, (e) *rac*-**5** with (*S*)-**3d**, (f) *rac*-**5** with (*S*)-**2**, (g) *rac*-**5** with (*S*)-**3b**, (h) *rac*-**5** with (*S*)-**3c**, and (i) *rac*-**5** with (*S*)-**3a** in 0.6 mL of chloroform-*d* at 25 °C. CH resonances of *rac*-**5** are highlighted in wine red colour box.

Table 2 Optimization of amounts of (*S*)-**3a** and *rac*-**5**[a]

Entry	Amount of (*S*)-**3a** (mmol)	Amount of *rac*-**5** (mmol)	$(\Delta\delta^{R/S})^b$ (ppm)
1	0.0125	0.05	0.02
2	0.025	0.05	0.03
3	0.05	0.05	0.04
4	0.1	0.05	0.06
5	0.1	0.0125	0.06
6	0.1	0.025	0.06
7	0.1	0.1	0.06

[a] In NMR tube, the CSA (*S*)-**3a** (0.0125–0.1 mmol) and *rac*-**5** (0.0125–0.1 mmol) were dissolved in chloroform-*d* (0.6 mL) and after shaking the NMR tube for 30 seconds, ^{1}H-NMR spectrum was recorded on a 400 MHz NMR spectrometer at 25 °C. [b] Calculated from the ^{1}H-NMR spectrum.

recorded in 0.6 mL of chloroform-*d* by gradually increasing the amount of (*S*)-**3a** as a chiral solvating agent (Table 2, entries 1–4 and see ESI, Fig. 1A†). The amount of (*S*)-**3a** was varied from 0.0125 mmol to 0.1 mmol with fixed amount (0.05 mmol) of *rac*-**5** and 0.1 mmol was found to be sufficient amount to get the clear baseline separation ($\Delta\delta^{R/S}$ = 0.06 ppm) of C<u>H</u> resonance of *rac*-**5**. Experiments were also conducted by varying the amount of *rac*-**5** from 0.0125 mmol to 0.1 mmol with fixed amount (0.1 mmol) of (*S*)-**3a** (Table 2, entries 4–7 and see ESI, Fig. 1B†). The 0.05 mmol of *rac*-**5** and 0.1 mmol of (*S*)-**3a** in 0.6 mL of chloroform-*d* was found to be the optimum amounts to get a clear baseline separation of C<u>H</u> resonance of *rac*-**5**. Fig. 2 (ESI†) shows that, as the amount of *rac*-**5** is increased from 0.0125 mmol to 0.1 mmol then observed broad singlet signal is upfield shifted from δ = 4.35 to 2.94 ppm. This clearly confirm the intramolecular hydrogen bond formation between OH and NH_2 groups of (*S*)-**3a** and *rac*-**5**, respectively.

To know the effect of temperature on enantiodifferentiation of 1,2-diphenylethylenediamine (**5**) using (*S*)-**3a** as a chiral solvating agent, the ^{1}H-NMR experiments were conducted at variable temperature (VT) in 0.6 mL of chloroform-*d*. The

Table 3 To study the effects of variable temperature (VT) on magnitude of $\Delta\delta^{R/S}$ of *rac*-**5**[a]

Entry	Temp. (°C)	Chemical shift difference $(\Delta\delta^{R/S})^b$ (ppm)	
		C<u>H</u>^{1}	C<u>H</u>^{2}
1	−50	0.52	0.15
2	−40	0.40	0.11
3	−20	0.19	0.05
4	−10	0.14	No resol.
5	0	0.11	No resol.
6	10	0.09	No resol.
7	25	0.06	No resol.

[a] In NMR tube, the CSA (*S*)-**3a** (0.1 mmol) and *rac*-**5** (0.05 mmol) were dissolved in chloroform-*d* (0.6 mL) and after shaking the NMR tube for 30 seconds, ^{1}H-NMR spectrum was recorded on a 400 MHz NMR spectrometer at variable temperatures. [b] Calculated from the ^{1}H-NMR spectrum.

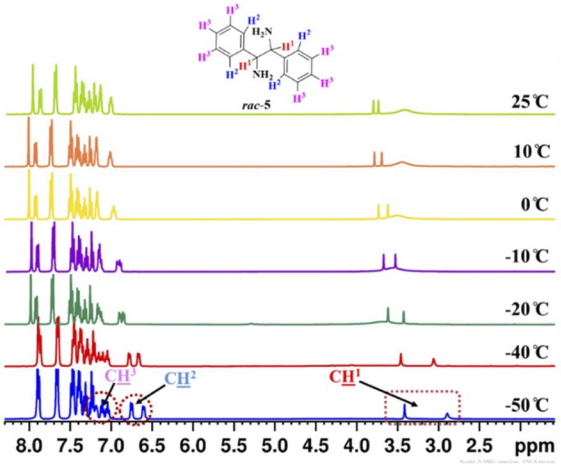

Fig. 3 Partial stacked plot of ^{1}H-NMR spectrum (400 MHz, $CDCl_3$) of *rac*-**5** (0.05 mmol) with (*S*)-**3a** (0.1 mmol) at variable temperatures in chloroform-*d* (0.6 mL). C<u>H</u>^{1}, C<u>H</u>^{2}, and C<u>H</u>^{3} resonances are highlighted in wine red colour box.

temperature was varied from 25 to −50 °C and at −50 °C very high chemical shift difference value ($\Delta\delta^{R/S}$ = 0.52 ppm) was observed for C<u>H</u>^{1} resonance of *rac*-**5**, because at low temperature the two enantiomers of 1,2-diphenylethylenediamine (**5**) reside in different local chemical environment for a longer time. At this temperature, even the aromatic proton signals for C<u>H</u>^{2} and C<u>H</u>^{3} of *rac*-**5** were also split into two distinct resonance peaks. The clear baseline separation was observed for C<u>H</u>^{2} resonance at −40 °C ($\Delta\delta^{R/S}$ = 0.11 ppm) and −50 °C ($\Delta\delta^{R/S}$ = 0.15 ppm) but C<u>H</u>^{3} resonance was overlapped in the aromatic ^{1}H-NMR region of (*S*)-**3a** (Table 3, and Fig. 3).

The reliability of the proposed protocol was evaluated by performing the experiments to measure the enantiomeric excess of 1,2-diphenylethylenediamine (**5**). The six different scalemic mixtures of enantiopure (1*R*,2*R*) and (1*S*,2*S*)-1,2-diphenylethylenediamine (**5**) (0.05 mmol) were prepared and their enantiomeric excess was determined by using (*S*)-**3a** (0.1 mmol) as a CSA in chloroform-*d* (0.6 mL) at 25 °C. The enantiomeric excess was calculated by integrating the C<u>H</u> resonance peaks observed for each of the enantiomers of 1,2-diphenylethylenediamine (**5**) from their respective ^{1}H-NMR spectrum (Fig. 4A). A linear relationship with a coefficient of R^2 = 0.9995 was observed between the theoretically calculated *ee* values and the *ee* values determined by ^{1}H-NMR spectra (Fig. 4B). These outcomes indicate, (*S*)-**3a** is an effective chiral solvating agent to determine the enantiomeric excess of 1,2-diphenylethylenediamine (**5**).

UV-visible spectroscopy is one of the best technique to study the extent of binding between both the enantiomers of analyte with CSA due to its easy handling and high sensitivity. Herein, we determine the binding constant for both the enantiomers of analyte **5** with CSA (*S*)-**3a**. Initially, the absorbance was measured for free CSA (*S*)-**3a** and then optically pure form of both the enantiomers of analyte **5** was added separately to get a two sets of readings. With the increase in equivalent of enantiomerically pure analyte **5**, the absorption intensity was

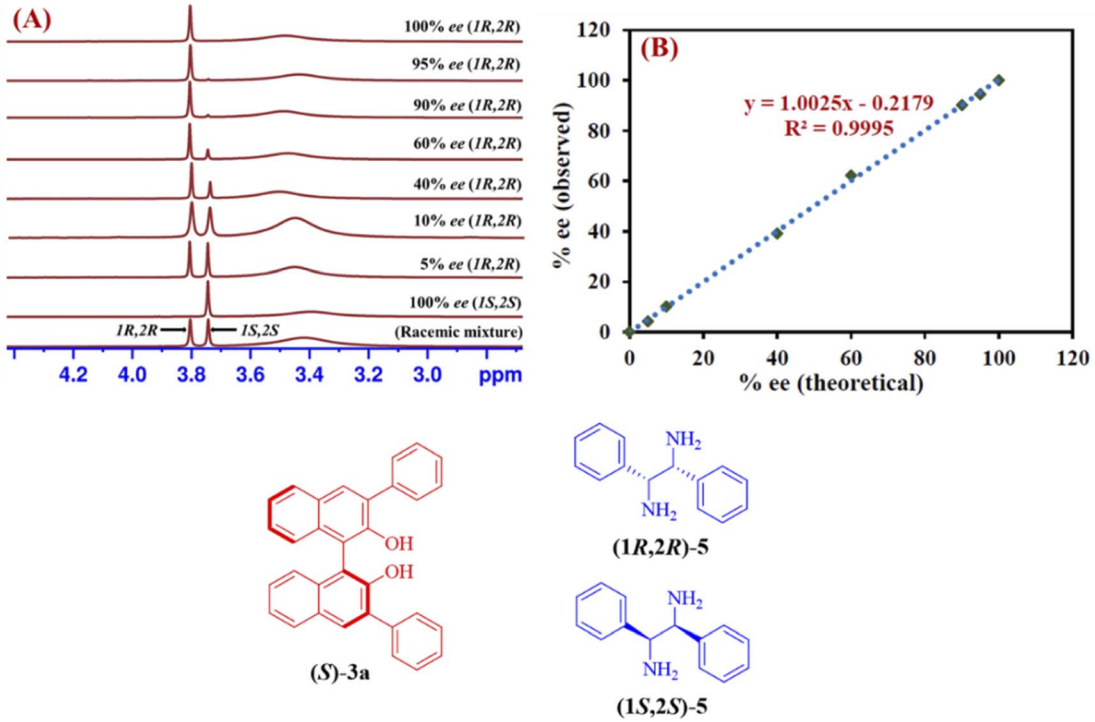

Fig. 4 (A) Partial stacked plot of ^{1}H-NMR spectrum (400 MHz, $CDCl_3$) for the CH resonance of **5** for six scalemic mixtures of enantiopure (1*R*,2*R*/1*S*,2*S*)-1,2-diphenylethylenediamine (**5**) with (*S*)-**3a** in 0.6 mL chloroform-*d* at 25 °C. (B) Linear relationship between theoretically determined *ee* values and the *ee* values determined by ^{1}H-NMR spectra.

also increased, which indicates the formation of diastereomeric host guest complex (see ESI, Fig. 3 and 4†). The change in the absorption intensity for both the enantiomers of analyte **5**, indicate their different extent of binding with CSA (*S*)-**3a**. A graph was plotted between the change in absorbance (ΔA) and the analyte concentration (C). The plot of $1/[\Delta A]$ *versus* $1/[C]$ gives a straight line with correlation coefficients (R^2) 0.99925 and 0.99743 for *R* and *S* enantiomers respectively (see ESI, Fig. 5†). The binding constants (K_R and K_S) for analyte **5** were calculated from the slope of the plot using modified Benesi–Hildebrand equation given below:[25]

$$\frac{1}{A - A_0} = \frac{1}{K_a} \times \frac{1}{C} + I$$

where A_0 is the absorbance of free CSA (*S*)-**3a** and A is the absorbance after addition of enantiomerically pure analyte **5** at concentration C.

The Gibbs free energy (ΔG) for diastereomeric complexes formed between CSA (*S*)-**3a** and both the enantiomer of analyte **5** were calculated from the binding constant (K_R/K_S) using following equation:

$$\Delta G = -RT \ln K$$

The calculated binding constant and ΔG values for diastereomeric complexes formed between both the enantiomers of analyte **5** with CSA (*S*)-**3a** are summarized in Table 4.

The results in Table 4 shows that the K_S value is more compared to K_R value for analyte **5**, which conclude that CSA (*S*)-**3a** form stronger diastereomeric complex with (*S*)-**5** compared to (*R*)-**5** enantiomer.

The NMR enantiodifferentiation of *rac*-2-amino-3-phenylpropan-1-ol (**6**) (0.025 mmol) with 0.1 mmol of CSAs **1**, and **3a–d** was evaluated in 0.6 mL of chloroform-*d* at 25 °C. The multiplet signal that appeared at 3.11 ppm for CH resonance of *rac*-**6** was separated into two distinct resonance peaks with a $\Delta\delta^{R/S}$ value of 0.09 ppm in the presence of (*S*)-BINOL (**1**) (Table 5 and see ESI, Fig. 6†). The ^{1}H-nuclei nearby to the amine group shows significant shielding due to the hydrogen bond formation between NH_2 and OH group of analyte **6** and two OH group of (*S*)-BINOL (**1**) and the diastereomeric host guest complexes were formed between (*S*)-BINOL (**1**) and two enantiomers of analyte **6**. No clear baseline separation was observed for the CH signal of analyte **6**, if 3,3-disubstituted (*S*)-BINOLs (**3a–d**) were

Table 4 The binding constant (K) and associated ΔG values for diastereomeric complexes formed between both the enantiomers of analyte **5** with CSA (*S*)-**3a**[a]

Substrate	K (L mol^{-1})	ΔG (kJ mol^{-1})
(*R*)-**5**	617.28	−15.91
(*S*)-**5**	900.90	−16.85

[a] Calculated from equation $\Delta G = -RT \ln K$, where R = 0.008314 kJ mol^{-1} K^{-1}, T = 298.15 K.

Table 5 Screening of various chiral solvating agents (CSAs) to determine the enantiodifferentiation of *rac*-**6**[a]

Entry	Chiral solvating agents (CSAs)	$(\Delta\delta^{R/S})^b$ (ppm)
1	(*S*)-**1**	0.09
2	(*S*)-**3a**	0.06
3	(*S*)-**3b**	0.05
4	(*S*)-**3c**	0.05
5	(*S*)-**3d**	No resol.

[a] In NMR tube, the CSAs (0.1 mmol) and *rac*-**6** (0.025 mmol) were dissolved in chloroform-*d* (0.6 mL) and after shaking the NMR tube for 30 seconds, ^{1}H-NMR spectrum was recorded on a 400 MHz NMR spectrometer at 25 °C. [b] Calculated from the ^{1}H-NMR spectrum.

Table 7 Optimization of molar ratio of (*R*)-**4** and *rac*-**8**[a]

Entry	Amount of *rac*-**8** (mmol)	$(\Delta\delta^{R/S})^b$ (ppm) CH	Ar-C$\underline{H}_3$	C$\underline{H}_3$
1	0.0125	No resol.	0.04	0.04
2	0.025	No resol.	0.05	0.05
3	0.05	No resol.	0.05	0.06
4	0.1	0.16	0.13	0.09
5	0.2	0.09	0.06	0.05

[a] In NMR tube, the CSA (*R*)-**4** (0.1 mmol) and *rac*-**8** (0.0125–0.2 mmol) were dissolved in chloroform-*d* (0.6 mL) and after shaking the NMR tube for 30 seconds, ^{1}H-NMR spectrum was recorded on a 400 MHz NMR spectrometer at 25 °C. [b] Calculated from the ^{1}H-NMR spectrum.

used as chiral solvating agents. This may be due to the steric repulsion exhibited by bulky substituents attached at 3,3′-position of (*S*)-BINOL to form the hydrogen bond between analyte **6** and CSAs. Therefore, (*S*)-BINOL (**1**) was found to be the effective chiral solvating agent for the NMR enantiodifferentiation of analyte **6**.

The effects of change in molar ratios of (*S*)-BINOL (**1**) and analyte **6**, were also studied for enantiodifferentiation of analyte **6**. With a fixed amount (0.1 mmol) of (*S*)-BINOL (**1**), the NMR experiments were performed by varying the amount of analyte **6** from 0.0125 mmol to 0.125 mmol (Table 6, entries 1–6, and see ESI, Fig. 7†). With 0.0125 mmol of analyte **6**, the maximum enantiodifferentiation ($\Delta\delta^{R/S} = 0.09$ ppm) was observed but the integration of resolved peaks for C$\underline{H}$ protons was found to be unequal. After then the amount of analyte **6** was increased from 0.0125 mmol to 0.125 mmol and best baseline separation and integration of resolved peaks for CH resonance was observed at 0.025 mmol of analyte **6**. Hence, 0.1 mmol of (*S*)-BINOL (**1**) and 0.025 mmol of analyte **6** in 0.6 mL of chloroform-*d* were found to be the optimum condition to get the clear baseline separation for C$\underline{H}$ resonance of analyte **6**.

We have also screened the (*S*)-BINOL derived chiral solvating agents to determine the enantiodifferentiation of secondary amines (**7–11**) and none of the BINOL derivatives showed separation of C$\underline{H}$ proton signals for secondary amines (see ESI, Fig. 8†). The (*R*)-1,1′-binaphthyl-2,2′-diyl hydrogenphosphate (**4**) undergoes a neutralization reaction with chiral amines and forms an ion-pair in chloroform-*d*, resulted in the separation of proton signals of analyte **7–11**.[19,54] Initially, we optimized the molar ratio of CSA **4** and analyte **8** to get a good enantiodifferentiation of secondary amines. With the fixed amount of CSA **4** (0.1 mmol), the amounts of analyte **8** were varied from 0.0125 mmol to 0.2 mmol (Table 7, entries 1–5, and see ESI, Fig. 9†) and results show that 0.1 mmol of CSA **4** and 0.1 mmol of analyte **8** was found to be optimal amount to get the clear baseline separation in analyte **8**. At this molar ratio, the maximum baseline separation for the C$\underline{H}_3$ ($\Delta\delta^{R/S} = 0.09$ ppm), aromatic C$\underline{H}_3$ ($\Delta\delta^{R/S} = 0.13$ ppm) and C$\underline{H}$ ($\Delta\delta^{R/S} = 0.16$ ppm) resonance of analyte **8** were observed (Table 7, entry 4). With a decrease in the amount of *rac*-**8**, the overlapping of C$\underline{H}$ and CH_2 resonances were observed and also the $\Delta\delta^{R/S}$ values of C$\underline{H}_3$ and aromatic C$\underline{H}_3$ resonances were lowered. If we increased the amount of *rac*-**8** from 0.1 mmol to 0.2 mmol, the decreased in $\Delta\delta^{R/S}$ value was observed. Hence, it is essential to find the optimum amounts of CSAs and analytes to accomplish a good splitting of signals and to avoid overlapping of signals.

To know the generality of this protocol, the enantiodifferentiation of different secondary amines (**7–11**) (0.1 mmol) was investigated using (*R*)-1,1′-binaphthyl-2,2′-diyl hydrogenphosphate (**4**) (0.1 mmol) as a chiral solvating agent in 0.6 mL of chloroform-*d* at 25 °C. ^{1}H-, ^{13}C-, and ^{19}F-NMR spectra

Table 6 Optimization of molar ratio of (*S*)-BINOL (**1**) and *rac*-**6**[a]

Entry	Amount of *rac*-**6** (mmol)	$(\Delta\delta^{R/S})^b$ (ppm)
1	0.0125	0.09
2	0.025	0.09
3	0.05	0.08
4	0.075	0.07
5	0.1	0.07
6	0.125	0.06

[a] In NMR tube, the (*S*)-BINOL (**1**) (0.1 mmol) and *rac*-**6** (0.0125–0.125 mmol) were dissolved in chloroform-*d* (0.6 mL) and after shaking the NMR tube for 30 seconds, ^{1}H-NMR spectrum was recorded on a 400 MHz NMR spectrometer at 25 °C. [b] Calculated from the ^{1}H-NMR spectrum.

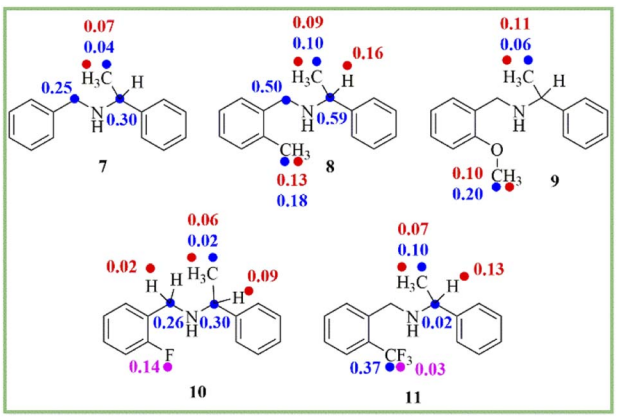

Scheme 2 The chemical shift difference ($\Delta\delta^{R/S}$) values of clearly baseline resolved proton (red), carbon (blue), and fluorine (pink) signals of secondary amines (**7–11**).

recorded for secondary amines are given in ESI (see ESI, Fig. 10–21†). The $\Delta\delta^{R/S}$ values of clear baseline resolved proton, carbon, and fluorine signals of secondary amines (**7**–**11**) are given in Scheme 2. As shown in ^{1}H-NMR spectrum (see ESI, Fig. 10†) of analyte **7**, the overlapping of C<u>H</u> and CH_2 resonances create inaccuracy in integrating the two distinct resonance peaks obtained for C<u>H</u> and CH_2 protons which led to inaccurate determination of enantiopurity of amines *via* ^{1}H-NMR spectroscopy.

In that case, the ^{13}C- and ^{19}F-NMR spectroscopy plays a crucial role to determine the enantiopurity of amines. The ^{13}C- and ^{19}F-NMR spectra were also recorded for secondary amines at 25 °C. The ^{19}F-NMR spectroscopy is also beneficial due to its 100% natural abundance and 83% signal sensitivity relative to ^{1}H-NMR spectroscopy and better separation of the signal due to less number of nuclei present in the analyte.[55] In this study, two examples of fluorine containing analytes (**10** and **11**) are included. The analyte **10** ($\Delta\delta^{R/S}$ = 0.14 ppm) shows more splitting of a signal as compared to analyte **11**, which is having CF_3 group ($\Delta\delta^{R/S}$ = 0.03 ppm) (see ESI, Fig. 18 and 21†).

Experimental

General procedure for NMR sample preparation

The analyte (0.0125–0.2 mmol) and chiral solvating agent (0.0125–0.1 mmol) were directly mixed in an NMR tube and dissolved in chloroform-*d* (0.6 mL). After shaking the NMR tube for 30 seconds, ^{1}H-, ^{13}C-, and ^{19}F-NMR spectra were recorded on a 400 MHz NMR spectrometer at 25 °C and well-resolved resonance peaks were observed for both the enantiomers present in an analyte. The enantiopurity was calculated by integrating the resonance peaks observed for each of the enantiomers of an analyte from their respective ^{1}H, ^{13}C-, and ^{19}F-NMR spectra.

Conclusions

In summary, a simple and fast protocol for enantiopurity determination of different types of amines (analytes) is described here *via* ^{1}H- and ^{19}F-NMR spectroscopy (for fluorinated analytes) in chloroform-*d* at 25 °C. (*S*)-**3a**, having phenyl group at 3,3′ positions act as a better CSA for NMR enantiodifferentiation of 1,2-diphenylethylenediamine while simple (*S*)-BINOL (**1**) shows better enantiodifferentiation for *rac*-2-amino-3-phenylpropan-1-ol. (*R*)-1,1′-Binaphthyl-2,2′-diyl hydrogenphosphate (**4**) acts as an effective chiral solvating agent for NMR enantiodifferentiation of different secondary amines. The enantiopurity of analyte **5** was determined and linear relationship with coefficient of R^2 = 0.9995 was observed. Using UV-visible spectroscopy, the binding constant and associated ΔG values were also calculated for diastereomeric complexes formed between both the enantiomers of analyte **5** with CSA (*S*)-**3a**. This protocol is very efficient and less time-consuming as compared to the derivatization protocol.

Author contributions

Pooja Chaudhary and Dr Geeta Devi Yadav were involved in the investigation, validation and data writing of this manuscript. Prof. Surendra Singh is involved conceptualization, funding acquisition, supervision of the research activity and writing of original draft of this manuscript.

Conflicts of interest

There are no conflicts to declare.

Acknowledgements

SS acknowledges the CSIR grant no. 02(317)/17/EMR-II. PC is thankful to CSIR for the Senior Research Fellowship (SRF). We are thankful to USIC, University of Delhi, Delhi, India for the instrumentation facility. We are also thankful to Synthesis with Catalyst Pvt. Ltd, India for gifting the (1*R*,2*R*)-1,2-diphenylethylenediamine and (1*S*,2*S*)-1,2-diphenylethylenediamine.

References

1 B. M. Trost and C. S. Brindle, *Chem. Soc. Rev.*, 2010, **39**, 1600–1632.
2 K. C. Nicolaou, J. S. Chen and S. M. Dalby, *Bioorg. Med. Chem.*, 2009, **17**, 2290–2303.
3 S. Mukherjee, J. W. Yang, S. Hoffmann and B. List, *Chem. Rev.*, 2007, **107**, 5471–5569.
4 R. Wohlgemuth, *Curr. Opin. Microbiol.*, 2010, **13**, 283–292.
5 J. A. Tao, G.-Q. Lin and A. Liese, *Biocatalysis for the pharmaceutical industry: discovery, development and manufacturing*, John Wiley & Sons, 2009.
6 T. C. Nugent, *Chiral amine synthesis: methods, developments and applications*, John Wiley & Sons, 2010.
7 T. C. Nugent and M. El-Shazly, *Adv. Synth. Catal.*, 2010, **352**, 753–819.
8 P. Metola, E. V. Anslyn, T. D. James and S. D. Bull, *Chem. Sci.*, 2012, **3**, 156–161.
9 M. O. Okuom, R. Burks, C. Naylor and A. E. Holmes, *J. Anal. Methods Chem.*, 2015, 865605.
10 P. J. Walsh, D. K. Smith and C. Castello, *J. Chem. Educ.*, 1998, **75**, 1459–1462.
11 A. Kaddoumi, M. N. Nakashima and K. Nakashima, *J. Chromatogr. B: Biomed. Sci. Appl.*, 2001, **763**, 79–90.
12 I. Ilisz, A. Aranyi, Z. Pataj and A. Peter, *J. Pharm. Biomed. Anal.*, 2012, **69**, 28–41.
13 V. Schurig and H.-P. Nowotny, *Angew. Chem., Int. Ed.*, 1990, **29**, 939–1076.
14 M. A. Shishovska and M. T. Stefova, *J. Chromatogr. Sci.*, 2012, **50**, 43–50.
15 F. Chen, B. Fang and S. Wang, *J. Anal. Methods Chem.*, 2021, 8821126.
16 G. Roskam, B. Velde, A. Gargano and I. Kohler, *LCGC Europe*, 2022, 353, pp. 83–92.
17 L. Liu, C. Ma, Q. He, Y. Huang and W. Duan, *Org. Chem. Front.*, 2021, **8**, 4144–4152.
18 D. Prasad, S. Mogurampelly and S. R. Chaudhari, *RSC Adv.*, 2020, **10**, 2303–2312.
19 B. Benedict, C. E. Lietz and T. J. Wenzel, *Tetrahedron*, 2018, **74**, 4846–4856.

20 S. H. Jung, K. Y. Kim, A. Ahn, S. S. Lee, M. Y. Choi, J. Jaworski and J. H. Jung, *New J. Chem.*, 2016, **40**, 7917–7922.
21 C.-X. Liu, L. Zheng, L. Zhu, H.-P. Xiao, X. Li and J. Jiang, *Org. Biomol. Chem.*, 2017, **15**, 4314–4319.
22 N. Jain, R. B. Patel and A. V. Bedekar, *RSC Adv.*, 2015, **5**, 45943–45955.
23 H. B. Raval and A. V. Bedekar, *ChemistrySelect*, 2020, **5**, 6927–6932.
24 R. Gupta, R. G. Gonnade and A. V. Bedekar, *J. Org. Chem.*, 2016, **81**, 7384–7392.
25 R. Gupta, R. G. Gonnade and A. V. Bedekar, *ChemistrySelect*, 2020, **5**, 13183–13190.
26 J. C. Merino, A. F. Keppler and M. S. Silva, *J. Braz. Chem. Soc.*, 2018, **29**, 1638–1644.
27 P. Borowiecki, *Tetrahedron: Asymmetry*, 2015, **26**, 16–23.
28 F. Yuste, R. Sánchez-Obregón, E. Díaz and M. A. García-Carrillo, *Tetrahedron: Asymmetry*, 2014, **25**, 224–228.
29 J. S. Salsbury and P. K. Isbester, *Magn. Reson. Chem.*, 2005, **43**, 910–917.
30 F. Toda, K. Mori, J. Okada, M. Node, A. Itoh, K. Oomine and K. Fuji, *Chem. Lett.*, 1988, **17**, 131–134.
31 S. K. Mishra and N. Suryaprakash, *Tetrahedron: Asymmetry*, 2017, **28**, 1220–1232.
32 L.-P. Li and B.-H. Ye, *Inorg. Chem.*, 2017, **56**, 10717–10723.
33 N. V. Orlov and V. P. Ananikov, *Green Chem.*, 2011, **13**, 1735–1744.
34 Y. Pérez-Fuertes, A. M. Kelly, J. S. Fossey, M. E. Powell, S. D. Bull and T. D. James, *Nat. Protoc.*, 2008, **3**, 210–214.
35 A. M. Kelly, S. D. Bull and T. D. James, *Tetrahedron: Asymmetry*, 2008, **19**, 489–494.
36 Y. Pérez-Fuertes, A. M. Kelly, A. L. Johnson, S. Arimori, S. D. Bull and T. D. James, *Org. Lett.*, 2006, **8**, 609–612.
37 H. J. C. Yeh, S. K. Balani, H. Yagi, R. M. E. Greene, N. D. Sharma, D. R. Boyd and D. M. Jerina, *J. Org. Chem.*, 1986, **51**, 5439–5443.
38 K. Omata, S. Aoyagi and K. Kabuto, *Tetrahedron: Asymmetry*, 2004, **15**, 2351–2356.
39 I. Ghosh, H. Zeng and Y. Kishi, *Org. Lett.*, 2004, **6**, 4715–4718.
40 J. Yi, G. Du, Y. Yang, Y. Li, Y. Li and F. Guo, *Tetrahedron: Asymmetry*, 2016, **27**, 1153–1159.
41 M. Ardej-Jakubisiak and R. Kawecki, *Tetrahedron: Asymmetry*, 2008, **19**, 2645–2647.
42 J. Redondo, A. Capdevila and I. Latorre, *Chirality*, 2010, **22**, 472–478.
43 G. Du, Y. Li, S. Ma, R. Wang, B. Li, F. Guo, W. Zhu and Y. Li, *J. Nat. Prod.*, 2015, **78**, 2968–2974.
44 W. H. Pirkle and D. J. Hoover, *Top. Stereochem.*, 1982, **13**, 263–331.
45 T. R. Wu, L. Shen and J. M. Chong, *Org. Lett.*, 2004, **6**, 2701–2704.
46 C. Recsei and C. S. P. McErlean, *Tetrahedron*, 2012, **68**, 464–480.
47 W. Hu, J. Zhou, X. Xu, W. Liu and L. Gong, *Org. Synth.*, 2011, **88**, 406–417.
48 Y. Liu, S. Zhang, Q. Miao, L. Zheng, L. Zong and Y. Cheng, *Macromolecules*, 2007, **40**, 4839–4847.
49 L.-J. Yan, X. Liu, P.-A. Wang, H.-F. Nie and S.-Y. Zhang, *Org. Prep. Proced. Int.*, 2013, **45**, 473–482.
50 W. Zhang, J. L. Loebach, S. R. Wilson and E. N. Jacobsen, *J. Am. Chem. Soc.*, 1990, **112**, 2801–2803.
51 P. Chaudhary, G. D. Yadav, K. K. Damodaran and S. Singh, *New J. Chem.*, 2022, **46**, 1308–1318.
52 J. H. Shim, M.-J. Kim, J. Y. Lee, K. H. Kim and D.-C. Ha, *Tetrahedron Lett.*, 2020, **61**, 152295.
53 M. Ratajczak-Sitarz, A. Katrusiak, K. Gawrońska and J. Gawroński, *Tetrahedron: Asymmetry*, 2007, **18**, 765–773.
54 J.-H. Tay and P. Nagorny, *Synlett*, 2016, **27**, 551–554.
55 S. Jang and H. Kim, *Org. Lett.*, 2020, **22**, 7804–7808.